DEVELOPMENTAL DYNAMICS 202:101–114 (1995)

Three-Dimensional Gradients of Voltage During Development of the Nervous System as Invisible Coordinates for the Establishment of Embryonic Pattern

RIYI SHI AND RICHARD B. BORGENS
Center for Paralysis Research, Department of Anatomy, School of Veterinary Medicine, Purdue University, West Lafayette, Indiana 47907-1244

ABSTRACT **We are interested in the generation of endogenous electric fields associated with ionic currents driven through the vertebrate embryo by the transepithelial potential of its surface ectoderm. Using a non-invasive vibrating electrode for the measurement of ionic current, we have provided measurements of currents traversing amphibian embryos, and a preliminary report of the internal, extracellular voltage gradient under the neural plate which polarizes the embryo in the rostral/caudal axis (Metcalf et al. [1994] J. Exp. Zool. 268:307–322). Here we complete a description of this gradient in electrical potential (ca. 10 mV/mm, caudally negative), describe a simultaneous gradient organized in the medial/lateral axis (ca. 5–18 mV/mm, negative at the margins of the neural folds), and describe their appearance and disappearance during ontogeny of the axolotl embryo. Both voltage gradients are not expressed until neurulation, and disappear at its climax. This appearance and disappearance correlates with the shunting of current out of the lateral margins of the neural folds in rostral regions of the embryo beginning at stage 15, and is not associated with a more substantial current leak from the blastopore which appears at gastrulation. A steady blastopore current is still present after neural tube formation when intra-embryonic electric fields have been extinguished. We discuss the direct experimental tests supporting the hypothesis that these extracellular electric fields both polarize the early vertebrate embryo and serve as cues for morphogenesis and pattern.**

Key words: Electric fields, Ionic current, Neurodevelopment, Neurula, Neural plate

INTRODUCTION

During early development, an unknown communication system is set up within the embryo that helps lay out the ground plan for somatic form. Over eighty years ago, Hans Driesch elegantly stated an observation—and a conclusion to be drawn from it—which has helped frame an era of investigation into the control of pattern formation during ontogeny.

> The relative position of a blastomere in the whole determines in general what develops from it; if its position is changed, it gives rise to something different. In other words, its prospective value is a function of its position. (Wilson, 1925)

This, of course, does not just apply to the position of blastomeres, but to other developing cells within a morphogenetic field. The concept of morphogenetic fields has in recent years fallen out of fashion. It describes, amongst several things, the phenomenon of an empirically defined expanse of embryonic tissue, with boundaries, within which cells demonstrate regulative ability. What type of informational system exists in the embryo that might direct cellular development based on a cell's position within such a field? It is clear that the activation of certain sets of genes (such as Wnt-1 and Hox-1 and 3 in the mouse embryo) and the products of such gene activation (such as TGFβ and Wnt-1 families of growth factors) may indeed provide cells with "positional information," and so define an understanding of how cellular differentiation may be focused down different routes by cells sharing a similar anatomy and location on the embryo (Jessell and Melton, 1992; O'Farrell, 1994). Gradients of growth factors (or transcriptional activators) have also been invoked to demonstrate how such differential gene activation may be spatially controlled (Anderson, 1992). Warner (1985) and her colleagues have provided evidence that physiological differences between adjacent embryonic cells produce real boundaries, and that these boundaries help define the developmental potential of cells residing within or without. In cells of the amphibian neural plate, a rise in resting potential is observed that is not characteristic of other adjacent ectodermal cells (Blackshaw and Warner, 1976). This appears to be related to increased numbers of Na^+ pumps inserted into their membranes as well as electrical coupling between neural plate cells separating this region from non-neural plate ectoderm. Inhibition of this increase in resting potential by strophanthidin leads to embryonic abnor-

Received June 6, 1994; accepted September 15, 1994.
Address reprint requests/correspondence to Richard B. Borgens, Center for Paralysis Research, School of Veterinary Medicine, 1244 VCPR, Purdue University, West Lafayette, IN 47907-1244.
The authors dedicate this article to the memory of Michael Solursh.

malities, particularly in the developing brain and eyes (Messenger and Warner, 1979; Warner, 1985). Here we are concerned with another possible physiological control of early development—polarized gradients of subectodermal voltage. Recently we have offered physiological measurements of a polarized ionic current traversing both anuran and urodele embryos (Fig. 1), as well as a preliminary description of the magnitude of voltage gradients associated with this ionic current (Metcalf, et al., 1994). The amiloride/novobiocin sensitive transepithelial potential (TEP) expressed across embryonic ectoderm is the electromotive force generating this current flow which in turn sets up such steady, polarized, electrical fields within the embryo (Metcalf et al., 1994; Metcalf and Borgens, 1994). Transembryonic electric fields are on the order of 10–70 mV/mm, well within the range of voltages known to induce both specific architectural changes and migratory behavior in cultured embryonic cells (Robinson, 1985, Nuccitelli, 1988, Borgens, 1992, Borgens et al., 1994). Here we provide a complete description of rostral/caudal and medial/lateral gradients of voltage within the embryo, and reveal the timing of the appearance and disappearance of these intra-embryonic electric fields.

RESULTS

Ontogeny of the Rostral/Caudal Gradient of Extracellular Voltage

Microelectrode sampling of the TEP did not reveal a rostral/caudal gradient of voltage beneath the neural plate midline prior to stage 15, after which time a subectodermal voltage gradient, strikingly negative at the caudal neural plate, was clearly evident (Fig. 2, Fig. 3A,C). This gradient became less apparent by stage 18, and is not apparent at all at stage 19. Because of the fusion of the neural folds along the midline, only the most rostral and caudal recording locations can be used at stage 19 (refer to inset, Fig. 2). In spite of this difficulty, we can with certainty state that there is no drop in electrical potential between the presumptive head and tail at this stage (Fig. 3C) as is clearly evident at earlier times. By plotting the average field strength over the entire embryo as well as the largest potential drop between any two sampling positions (ca. 200–300 μm) for each stage, we determined this voltage gradient to be on the order of 10 mV/mm over the entire length of the ca. 2–2.7 mm long embryo (Table 1). It can, however, approach 75 mV/mm over shorter expanses (ca. 0.3 mm) beneath the neural plate (Fig. 4A). By plotting the percentage of embryos possessing the steepest potential drop over 300 μm by stage, it is also apparent that the locale of the largest recorded potentials shifts on the embryo with development (Fig. 4B). When there is little evidence of a rostral/caudal gradient over the length of the embryo (stage 14), the region where any potential drop exists at all is confined to subectodermal region of the caudal neural plate. Once a strong and steady rostral/caudal gradient is expressed over the length of the embryo, the locale of the steepest potential drop becomes localized to the middle to rostral subectodermal region in 75% of the embryos. When the rostral/caudal gradient begins to disappear (stage 18), the caudal region of subectodermal neural plate becomes, once again, the region where any potential drop that might occur would likely be detected (Fig. 4B). Electrical measurements made in stage 16 axolotls were entirely consistent with the preliminary voltage gradients previously reported (Metcalf et al., 1994).

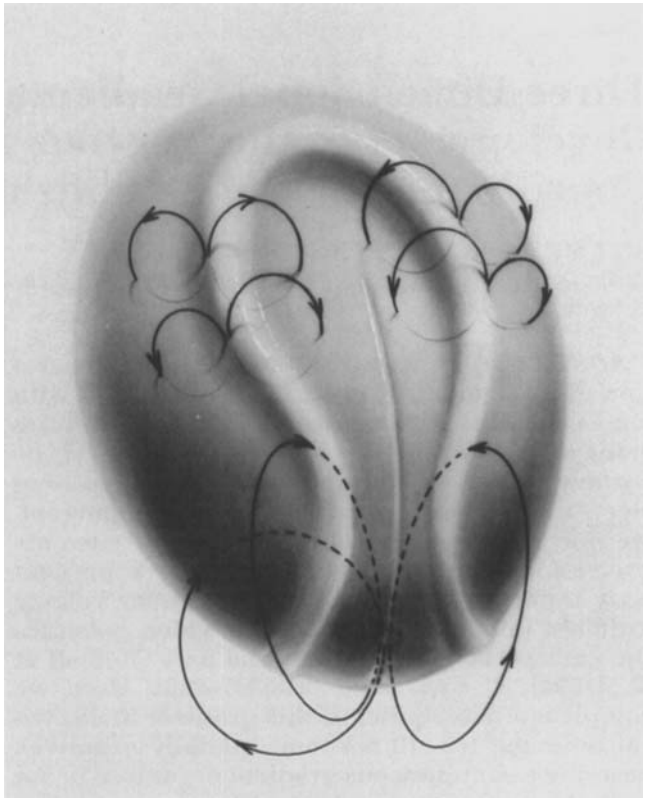

Fig. 1. Ionic currents traverse amphibian embryos. Spatially organized patterns of a steady ionic current are driven through the urodele and anuran embryo during neurulation. Current is driven out the lateral margins of the neural folds and out of the blastopore, returning through the general body surface. The battery driving this current out of the embryo is the inwardly positive transepithelial potential (ca. 20–50 mV) of embryonic ectoderm (Metcalf et al., 1994). Since the direction of current flow in biological systems is defined as the direction in which positive charges move, net ionic current leaks out of ectodermal regions of low electrical resistance. This current can be detected non-invasively with a vibrating electrode positioned near, but not touching, the embryo (Jaffe and Nuccitelli, 1974; Metcalf et al., 1994).

In summary, a drop in voltage of about 10 mV/mm, negative in caudal extracellular regions beneath the neural plate ectoderm with respect to rostral regions, begins to appear early during neurulation (stage 15), and disappears completely just prior to neural fold fusion (stage 19). Furthermore, the locale of the largest electric fields beneath the neural plate shifts from caudal regions to the presumptive cranial enlargement

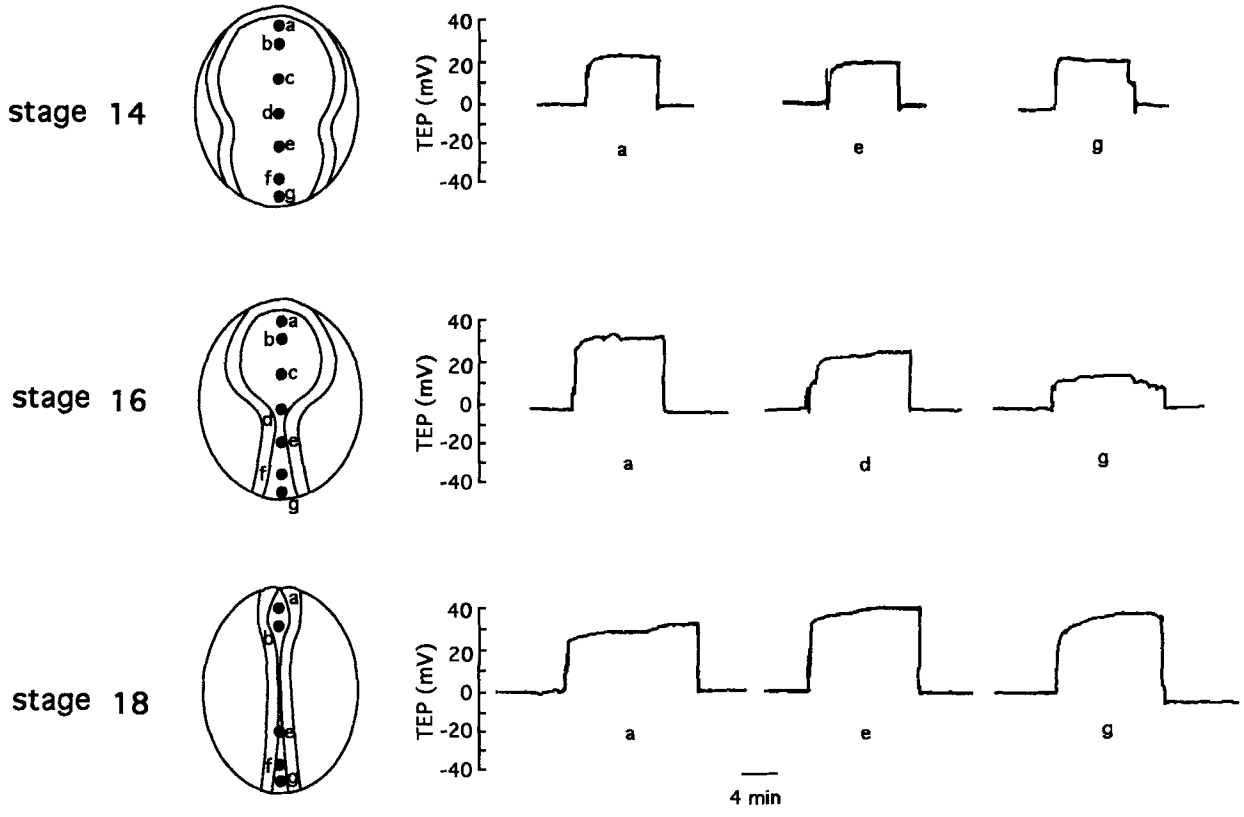

Fig. 2. Representative measurements of TEP along the neural plate midline. The embryonic stage and all standard microelectrode sampling positions for that stage are given to the left of three representative electrical records of TEP. All three records were obtained from the same embryo at the positions marked. Positions a and b, as well as f and g, were approximately 200 μm apart. The other positions were approximately 400 μm apart. Position g was approximately 100 μm from the blastopore. At stage 18 the loss of two sampling positions was caused by the dorsal fusion of the neural folds at that location. Note that all TEPs are inwardly positive with respect to the bath. Note as well the lack of an appreciable fall in potential from the rostral recording positions to the most caudal positions at stage 14 and 18. The stage 16 embryo demonstrates a typical fall in potential (in this case about 20 mV) along the rostral/caudal axis.

during neurulation in most embryos, and back again at the climax of neurulation. Table 1 provides physiological data derived from 280 TEP measurements in 48 embryos providing the data discussed above.

Transverse Voltage Gradients

Measurements along the transverse plane also revealed a gradient of voltage sampled along imaginary lines perpendicular to the long axis of the embryo. Eleven measurement locations per side along these axes were used at stage 15/16, and at the rostral, middle and caudal region of the embryo (Fig. 5). At stage 18/19, ten locations were sampled perpendicular to the long axis of the embryo, but only at two regions (rostral and caudal) since the neural folds had fused along the middle region of the embryo by this time. Figure 5 shows sample measurements at these locations at stages 15/16 and 18/19, for the right side only. An identical series of measurements was performed for the left side in an identical set of embryos. These measurements were technically more difficult and time consuming, thus during the course of any one measurement period, developmental stages graded into each other. Therefore we group these data into two periods during neurulation, stages 15/16 and 18/19 (just prior to neural fold fusion). Table 2 presents the numbers, locations, and field strengths for over 340 TEP measurements made in 32 embryos along these axes. At stage 15/16, rostral regions of the central neural plate are significantly higher in potential (more positive) than the lateral margins of the neural folds, resulting in field strengths as high as 18 mV/mm over this short distance (ca. 0.5 mm) (Fig. 6A). This fall in potential along the transverse axis is not evident at middle or caudal regions of the embryo at this stage (Fig. 6B, C). By stage 18/19, TEP values are not any lower in magnitude than at earlier stages of development, in fact they are generally larger as the TEP of amphibians increases in magnitude with developmental stage (Shi and Borgens, 1994; McCaig and Robinson, 1982). However, the distribution of TEPs at later developmental stages is more homogeneous and a depression in voltage at the margin of the neural folds is not as evident in rostral regions, while caudal regions of subectoder-

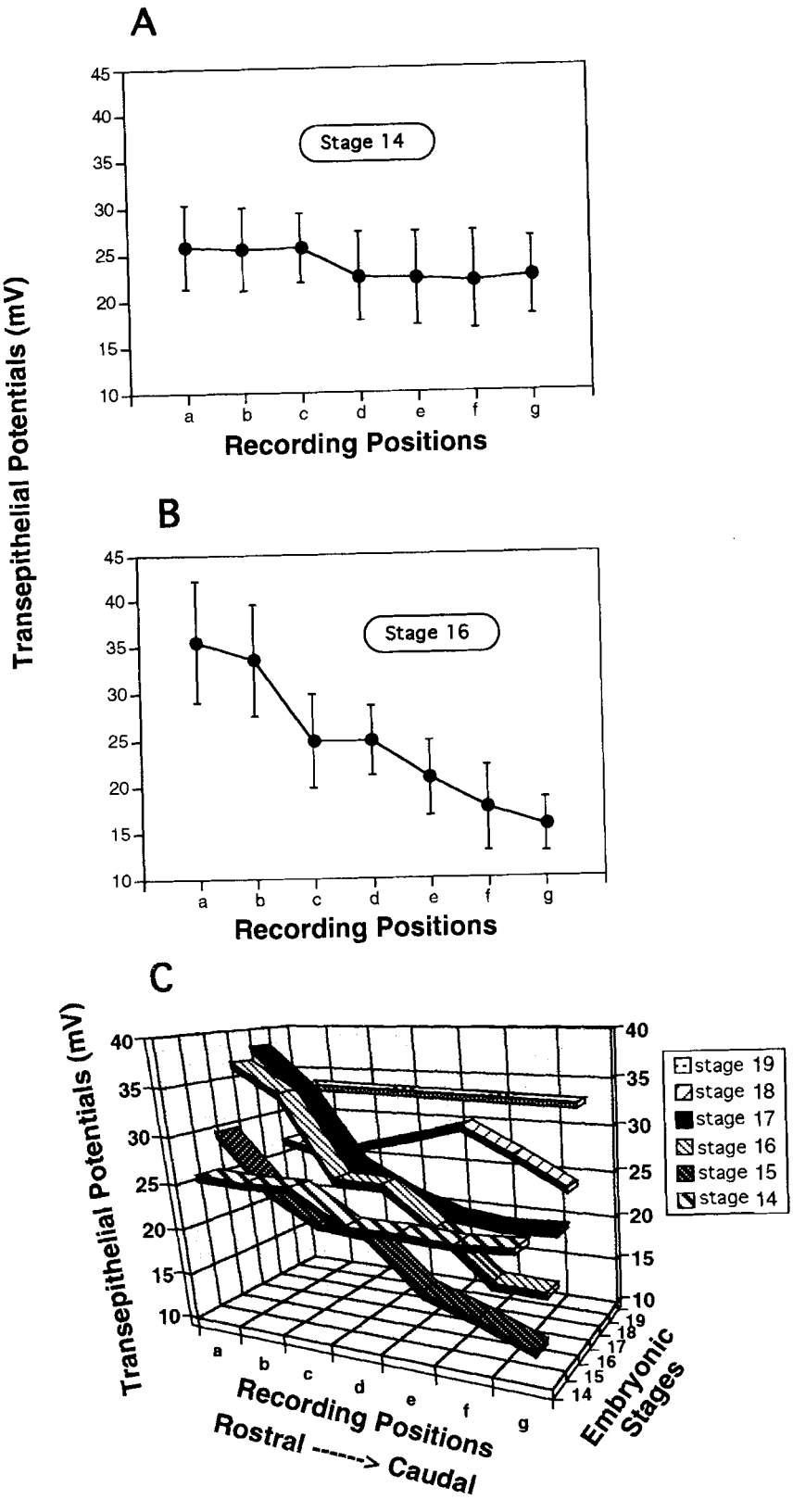
A
Stage 14
Transepithelial Potentials (mV)
Recording Positions
B
Stage 16
Recording Positions
C
Transepithelial Potentials (mV)
Recording Positions
Rostral ------> Caudal
Embryonic Stages
stage 19
stage 18
stage 17
stage 16
stage 15
stage 14

Fig. 3.

TABLE 1. Summary of Voltage Measurements in the Rostral/Caudal Axis

Stage	Number of embryos	TEP measurements per embryo	Mean lowest and mean highest TEP (mV)[a]	Slope or field strength (mV/mm)[b]	Field polarity[c]	*P* value of TEP comparison*
14	8	7	19–28	2.5	+	0.1
15	8	7	10–30	9.7	+	<0.01
16	8	7	13–37	10.8	+	<0.005
17	8	7	16–40	10.7	+	<0.005
18	8	5	21–32	2.3	+	0.35
19	8	2	31–35	1.5	+	0.78

[a]The lowest and highest average potential measurements are given for all embryos. These means do not correspond to any particular measurement position, but reflect the range of magnitudes observed at each stage.
[b]This value reflects the average field strength over the length of the embryo (most rostral to most caudal measurement positions). The embryos increase in length from about 2 mm at stage 14 to 2.7 mm by stage 19.
[c]In every case, the rostral subectodermal region of the neural plate was positive (+) with respect to caudal measurement positions.
*Rostral and caudal means were evaluated statistically (Student's t test, two tailed). Note that the rostral and caudal values are only significantly different at stages 15, 16, and 17.

mal voltage appear isopotential as in the preceding embryonic stages (Fig. 7).

Three-Dimensional Reconstruction of Voltage Gradients at Stages 15/16 and 18/19

The mean TEPs for all measurement locations was plotted against the rostral/caudal and transverse axes (Fig. 8). Such a plot emphasizes the steep fall in potential from the rostral midline to the left and right margin of the neural folds, and a more graded rise in potential as recordings are made more laterally to the flank. At caudal regions of the embryo, this topography of extracellular voltage is detectable, but barely so, given the more negative neural plate TEPs (with reference to rostral neural plate regions) combined with *more positive* TEPs at the *outside edge of the neural folds*. Prior to closure of the neural folds at stage 18/19, the embryo is not yet isopotential beneath the ectoderm; however, the striking voltage profiles have all but vanished (Fig. 9). The three-dimensional plot provided for stages 18/19 (Fig. 9, top graph) is not entirely comparable to that at stages 15/16 (Fig. 9, bottom graph), since some medial TEP position measurements were not made, given the fusion of the folds along the midline. This extrapolated topography, however, is statistically weighted for distance (refer to Experimental Procedures, below). Even though overall TEPs are larger in magnitude (at stage 18/19) than at earlier stages, the extracellular voltage gradients beneath the ectoderm appear more isopotential and there is little evidence of a marked internal electric field in any dimension.

Blastopore Measurements

To demonstrate that the appearance and disappearance of the gradients of extracellular voltage beneath the neural plate (especially in the rostral/caudal axis) *does not correlate* to outwardly directed ionic current at the blastopore (refer to Metcalf et al., 1994), we provide data collected from 7 embryos using an extracellular vibrating electrode (Metcalf and Borgens, 1994) at stages 17–24 (Fig. 10). By stage 19, the rostral/caudal voltage gradient beneath the neural plate ectoderm is extinguished (as described above); however, a steady blastopore current was observed in all seven embryos (refer also to blastopore measurements in Metcalf et al., 1994; and Robinson and Stump, 1984). We present these records to emphasize the presence of a steady, outwardly directed blastopore current existing well *after* closure of the neural folds and the simultaneous disappearance of both the rostral/caudal and medial/lateral voltage gradients within the embryo.

DISCUSSION

How Are Polarized Ionic Currents and Voltages Produced Within the Embryo?

Epithelial syncytia share certain physiological features with the ectodermal covering of the embryo. An epithelium possesses a potential difference across itself, the transepithelial potential or TEP. This potential usu-

Fig. 3. Distribution of TEPs along the neural plate midline. Representative mean and SEMs for eight stage 14 (**A**) and 16 (**B**) embryos (refer to Table 1). The measurement positions displayed along the abscissa are the same as those presented within the icons in Figure 2. Note the steep fall in potential along the rostral/caudal axis at stage 16. Mean TEPs recorded from rostral and caudal recording positions were not significantly different at stage 14 (refer to Table 1). A three dimensional graph (**C**) plots the magnitude of the mean TEP against the rostral/caudal recording positions and stage of development for all embryonic stages studied. Please recall the loss of central recording positions due to the fusion of the neural folds along the midline (refer to Experimental Procedures). Note the fall in potential between the rostral and caudal subneural plate ectoderm is only evident during stages 15–17. Only at these times are the recorded potentials at different ends of the embryo significantly different (refer to Table 1).

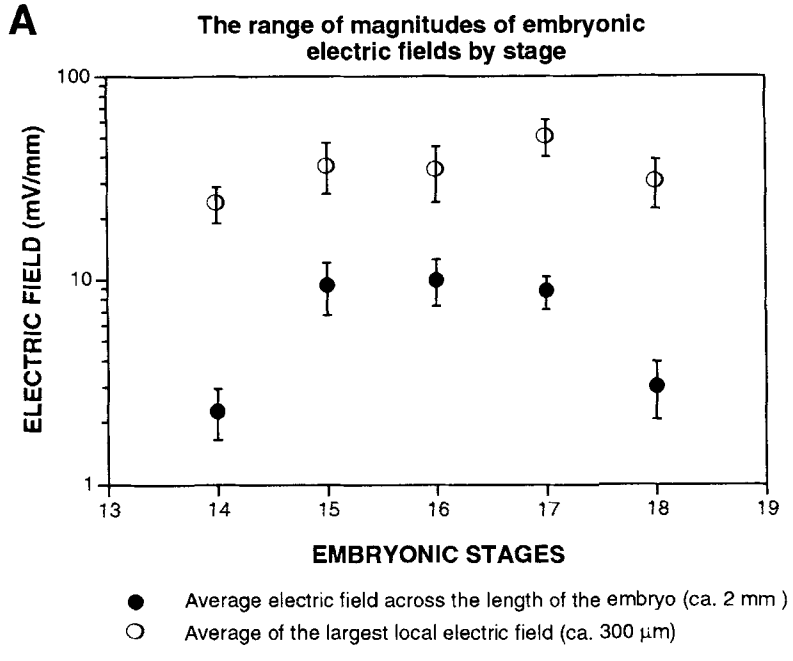

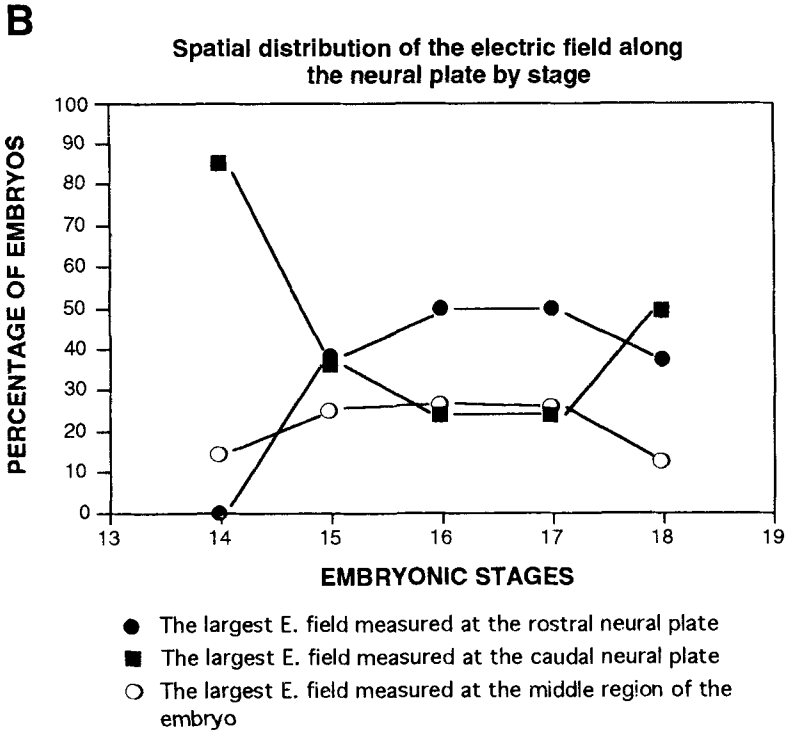

Fig. 4. Range and spatial distribution of subectodermal electric fields by embryonic stage. In **A** the mean voltage gradient and SEM over the length of eight embryos (ca. 2 mm; filled circle) or local region of highest field between two recording positions (ca. 300 μm; open circle) are displayed for stages 14–18 (refer to Table 1). The scale is logarithmic to allow the relatively high local voltage gradients to be displayed with the comparatively weaker electric fields measured over the embryo's length. Note that local fields may approach 70 mV/mm, while the weaker voltage gradients across the length of the embryo (ca. 10 mV/mm) are only observed during the process of neurulation, falling off with the beginning of neural fold fusion at stage 18. In **B**, the occurrence within the population of the largest local electric field at rostral, middle, and caudal regions under the neural plate is shown by stage. Note that at stage 14 and 18, the potential drop that could be detected (Figs. 2, 3a,c, Table 1) was observed in caudal subectodermal neural plate in the bulk of embryos studied. When the rostral/caudal voltage gradient is well expressed over the long axis of the embryo (stage 15–17) the region of the largest electric field shifts to the rostral region, the balance split between middle and caudal regions of the embryo.

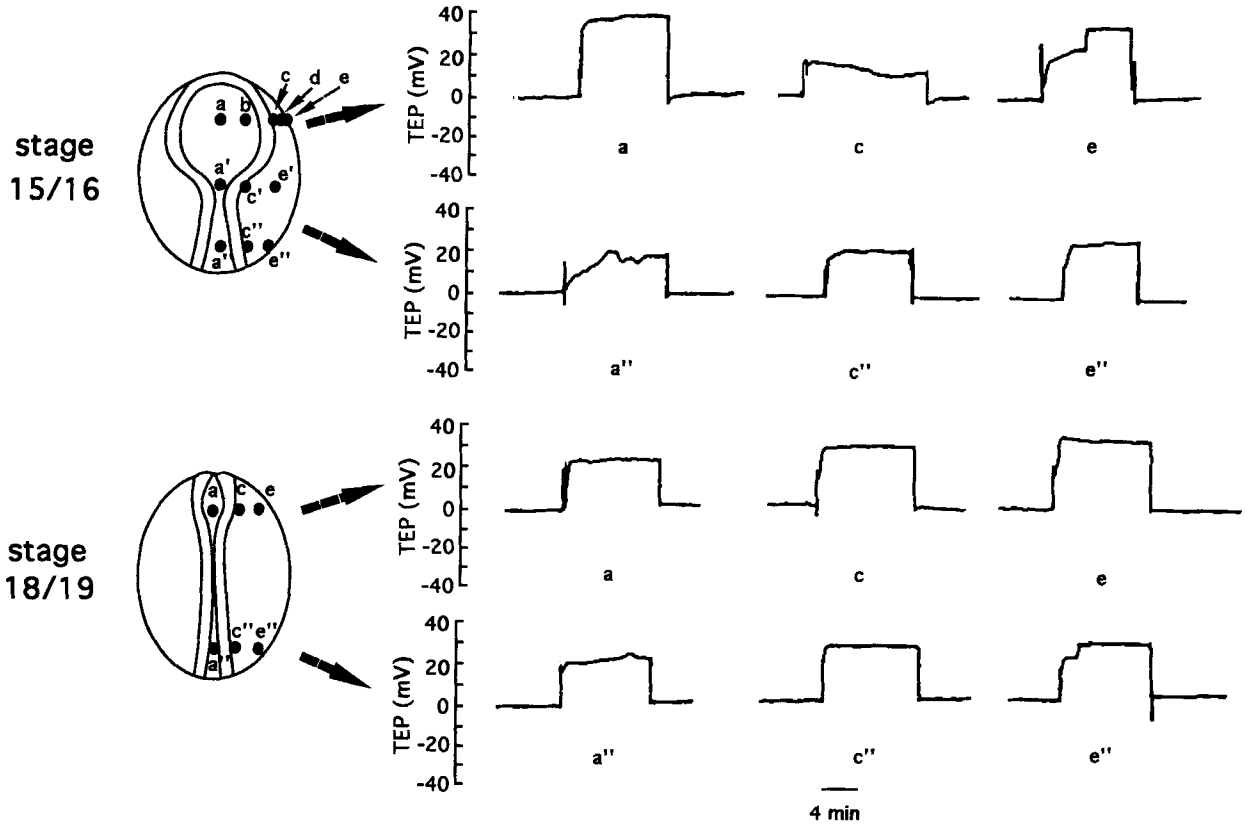

Fig. 5. Representative TEP measurements in the transverse axis with stage of development. The embryonic stage and all standard sampling positions for that stage are given to the left of three representative electrical records (refer to Fig. 2). All three records were obtained from the same embryo at the positions marked (only midline and right hand positions shown, left position measurements were also obtained from each embryo, Table 2). At stages 15/16, positions a, b, c, d, and e were approximately 250 μM apart; a, a', and a'' were approximately 800 μM apart; a' and c' and a'' and c'' were approximately 500 μM apart; and c' and e' were approximately 500 μM apart. At stage 18/19, a, c, and e were approximately 500 μM apart; a'', c'', 500 μm; and c'' and e'' 500 μM apart. Because of the close approximation of the lips of the neural folds in central and caudal regions, only 3 recording positions were used to span an equal distance relative to rostral regions. As in Figure 3, the fusion of the neural folds eliminated central recording positions at stages 18 and 19. Note the depression in TEP at the margin of the rostral neural fold (position c) but not at more caudal regions (c' and c'') at stages 15/16. Note the stage 18/19 embryo is isopotential in the transverse axis. The only statistically significant depression in TEP was observed at stages 15/16 and always in the rostral neural plate.

ally arises by a multi-step process first depending on the facilitated uptake of Na^+ through unique Na^+ channels restricted to the apical membranes (Kirschner, 1983; Smith and Benos, 1992). These channels should not be confused with the voltage dependent Na^+ channels of, typically, excitable cells such as nerve and muscle. They are blocked specifically by agents such as amiloride and its analogs, benzamil, ethylisopropyl amiloride, and the methyl ester of lysine. Na^+ is pumped out of basal membranes of epithelial cells into the extracellular space by typical Na^+/K^+ exchange producing TEPs ranging from 20 to 80 mV. Inwardly positive TEPs have been measured in amphibian blastula, gastrula, and neurula stage embryos, in primitive streak, and later stages of development in the chick, and have been strongly suggested by inward directed currents in mouse blastomeres, as well as by single cells of rabbit preimplantation trophoblast cells (Regen and Steinhardt, 1986; McCaig and Robinson, 1982; Metcalf and Borgens, 1994; Jaffe and Stern, 1979; Stern and MacKenzie, 1983; Wiley and Nuccitelli, 1986; Robinson et al., 1991). Furthermore, this TEP is capable of driving steady ionic current through, and out of, the embryo at regions of low electrical resistance. Since by convention we describe the direction of current flow to be the direction in which positive charge moves, the inwardly positive TEP would drive outwardly directed currents through low resistance regions, such as the blastopore, or the lateral margin of the neural folds (Metcalf et al., 1994). Here the electrical resistance of the ectoderm is compromised by tight junction dissolution during the remodeling of embryonic form during neurulation (Decker, 1981).

Intraembryonic Electric Fields in the Axolotl

Since the internally positive TEP drives current out of regions of low resistance such as the neural fold margins (Metcalf et al., 1994), we should expect that the TEP would be depressed here—which it is. The slope of the voltage gradient—or electric field—is both sub-

TABLE 2. Summary of Voltage Measurements in the Medial/Lateral Plane

Stage	Location of measurements[a]	Number of embryos	Number of measurement positions per embryo[b]	Average TEP range (mV)	Va + Ve/2 − Vc or average TEP depression in mV at edge of neural folds[c]	Slope or field strength of neural folds (mV/mm)[d]	*P* value of TEP comparison: midline vs. edge of neural fold	*P* value of TEP comparison: flank vs. edge of neural fold*
15/16	Rostral, midline-right	10	5	11–17	9	18	<0.0005	<0.005
	Middle, midline-right	10	3	14–17	3.5	7	0.23	<0.01
	Caudal, midline-right	10	3	13–19	0.5	1	0.83	0.35
	Rostral, midline-left	10	5	12–23	8	16	<0.01	<0.05
	Middle, midline-left	10	3	14–21	1.5	3	0.89	0.29
	Caudal, midline-left	10	3	13–18	0.5	1	0.78	<0.05
18/19	Rostral, left-right[e]	12	5	21–29	Right: 2.5	5	0.06	<0.05
					Left: 1.5	3	0.3	0.18
	Caudal, left-right[e]	12	5	19–26	Right: 0.5	1	0.38	0.4
					Left: 0.5	1	0.4	0.06

[a]Measurement positions are grouped as they were recorded in individual embryos at stage 15/16 and stage 18/19 (refer to Figs. 5, 6, and 7). Identical sets of embryos were evaluated at the neural plate midline to right flank, and neural plate midline to left flank (only right-hand measurement positions are depicted in the icon within Fig. 5—refer to Experimental Procedures).
[b]Note fewer recording positions in middle to caudal regions that span an equal distance to those in rostral regions of the embryo (refer to Fig. 5 legend) at stage 15/16. Note loss of central recording positions at stage 18/19 due to the fusion of the neural folds here.
[c]This depression in voltage was evaluated using the formula Va + Ve/2 − Vc, where Va = average magnitude of voltage for all embryos at position a (most rostral neural plate midline, refer to Fig. 5), Ve = average magnitude of voltage for all embryos at position e (most lateral flank measurement, refer to Fig. 5), and Vc = average magnitude of voltage measured in all embryos at position c (the lateral edge of the neural fold, refer to Fig. 5).
[d]The field strength is calculated using combined values recorded at a (midline) and e (lateral to the neural folds) with reference to c (the depressed voltage at the margin of the neural folds) divided by this measured distance.
[e]All measurements (left, midline, and right) were made on each embryo (refer to legend, Fig. 5).
*Note the TEPs recorded at the edge of the neural folds relative to adjacent flank are statistically significant in rostral regions but are not in middle or caudal regions of the embryo.

stantive (up to 18 mV/mm) and steady during neurulation. Thus, a medial to lateral electric field exists between the midline of the neural plate and the margin of the neural folds—but only in rostral regions of the embryo. At present, we have no clue why this profile is not as evident in caudal regions of the neural plate and folds. Perhaps tight junctional integrity is less disturbed here in some manner related to the way cells and sheets of cells may remodel in caudal regions of the neural plate. At the climax of neurulation this electric field disappears.

One would expect as well that the TEP of caudal regions of the neural plate (and adjacent ectoderm) to be more electrically negative than rostral regions because of the outwardly directed current at the blastopore. However, we do not believe the electric field beneath the neural plate is *related to the presence of the blastopore current* for the following reasons: 1) This current is present from the blastopores' formation during gastrulation, yet a marked rostral/caudal voltage gradient does not appear until early neurulation. 2) The disappearance of the rostral/caudal voltage gradient beneath the neural plate does not correlate with either a reduction or loss of the blastopore current—it persists well after neural tube formation in both anuran and urodele embryos (these data; see also Robinson and Stump, 1984). 3) The appearance and disappearance of the rostral/caudal voltage gradient does, however, correlate with the appearance and disappearance of the neural fold outcurrents. We believe it possible that some feature of internal resistance may change during neurulation, segregating the subneural plate region of ectoderm from the gut. For example, increasing junctional resistance between cells of the caudal archenteron wall might provide a preferential pathway for the blastopore shunt current, while buffering the TEP of overlying caudal ectoderm from the effects of that shunt current. Said another way, the embryo may be divided into two tiers, an upper region of subneural plate ectoderm where the magnitude of the TEP is more dependent on junctional changes at the walls of the neural folds, and a lower tier where current emerging from the blastopore is more controlled by junctional changes in the archenteron wall—diminishing any effect of this leakage current on the electrical potential across caudally located surface ectoderm.

In summary, the neurula is partitioned by a medial/lateral and a rostral/caudal gradient of voltage. The vector of these electric fields would be aligned in the dorsal/ventral axis, and altogether these extracellular voltages may provide a three dimensional coordinate system helping to specify early developing form (Fig. 11).

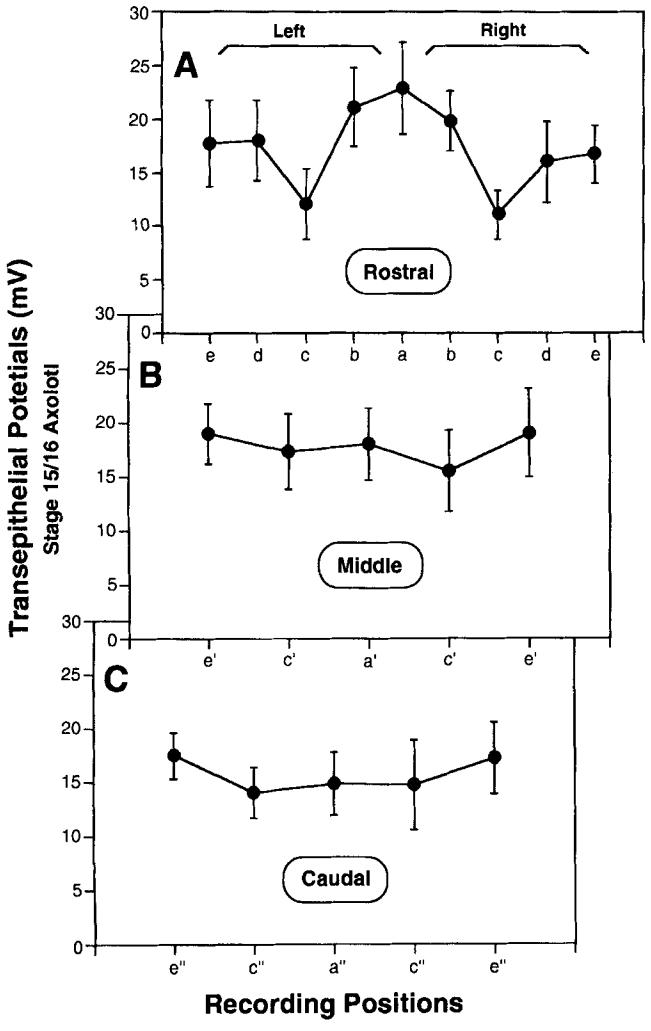

Fig. 6. Mean TEPs and their standard errors in the transverse axis at rostral (**A**), middle (**B**), and caudal (**C**) regions of the stage 15/16 embryo. Note the marked (and statistically significant) depression in TEP at position c, both left and right of the midline in rostral regions of the neural plate (refer to measurement positions marked in upper icon, Fig. 5). Note the lack of any such TEP depression at more caudal sampling positions. Each graph depicts the mean and SEM of measurements made in 20 embryos (Table 2).

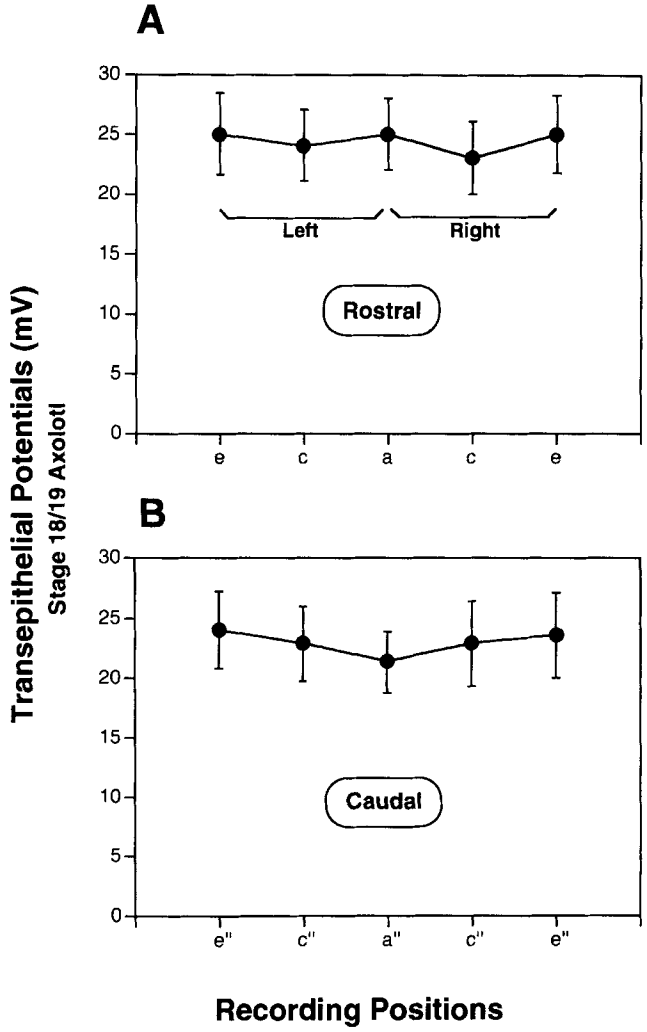

Fig. 7. Mean TEPs and their standard errors in the transverse axis at rostral (**A**) and caudal (**B**) regions of the stage 18/19 embryo. Note the lack of any significant depression in TEP at either the most rostral or caudal sampling positions. Measurement positions were identical for left and right sides (refer to lower icon, Fig. 5). Each graph depicts the mean and SEM of measurements made in 12 embryos (Table 2).

Are Endogenous Electric Fields an Epiphenomenon?

If the notion that a coordinate system of internal voltages may help lay out early somatic form is true, at least five corollaries must be satisfied: 1) embryonic cells must be responsive to extracellular voltages within the range of magnitudes measured within embryos, 2) disturbance of these endogenous gradients of voltage by *imposed voltages in the physiological range* should result in developmental arrest or abnormality, 3) this disturbance should be most profound at the embryonic stages when endogenous fields are present within the embryo, 4) since the internal voltages are spatially polarized during development, the form of teratological change in the embryo produced by an artificially imposed field should be predictable based on its orientation relative to the embryo's orientation, and 5) any technique that will reduce or eliminate an endogenous voltage gradient should lead to developmental arrest or retardation. All five of these requirements have been met.

1. It is already clear that embryonic cells in vitro such as neuroblasts, early neurons and their processes (Hinkle et al., 1981; Patel and Poo, 1982; McCaig, 1986), myoblasts and their processes (Hinkle et al., 1981, McCaig and Dover, 1989), embryonic fibroblasts (Erickson and Nuccitelli, 1984), and neural crest (Stump and Robinson, 1983; Cooper and Keller, 1984)

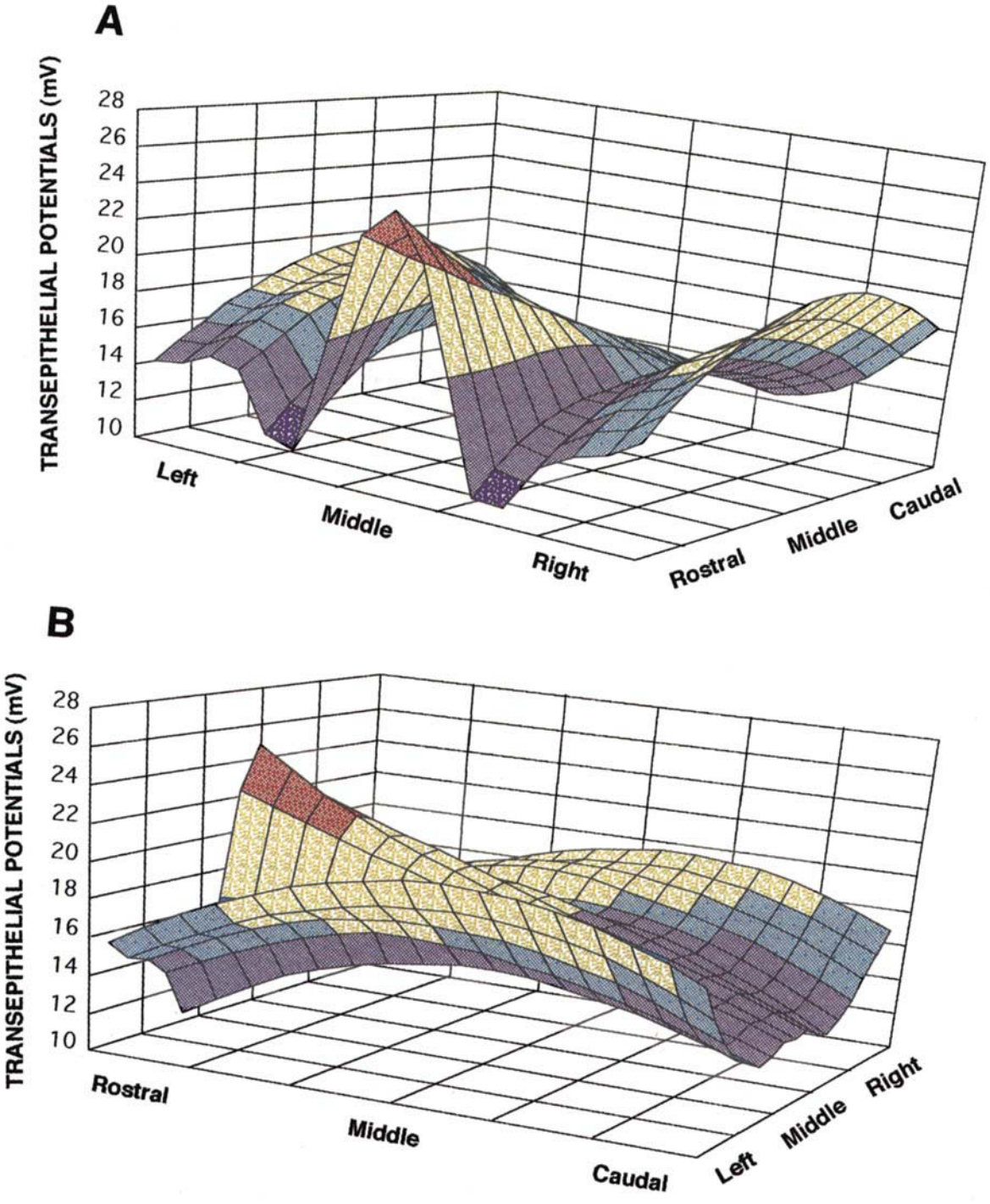

Fig. 8. Three-dimensional plot of the magnitude of TEPs at rostral/caudal and transverse axes at stage 15/16. The mean TEPs for all embryos are plotted. Two views of the same data are presented to provide the topography of voltage as seen from the front (**A**) (emphasizing both left and right profiles) and from the side (**B**) (emphasizing the rostral to caudal profile). A range of potential difference (in mV) is given by color: red = 19–25; yellow = 15–22; blue = 13–18; violet = 11–13; and dark violet = 10–12. Note the steep rostral/caudal (caudally negative) voltage gradient and the steep medial/lateral gradient (negative at the margins of the neural folds) of voltage at this stage of development.

realign themselves or migrate within imposed voltage gradients on the order of 1–100 mV/mm (reviewed by Nuccitelli, 1988; and Borgens, 1992). This is clearly within the range of measured endogenous voltages in embryos.

2. Imposed voltage gradients in the range reported here (25–75 mV/mm) severely disturb axolotl development compared to sham treated controls. These artificially imposed voltages were oriented in such a way as to reduce, enhance, or otherwise disturb endogenous

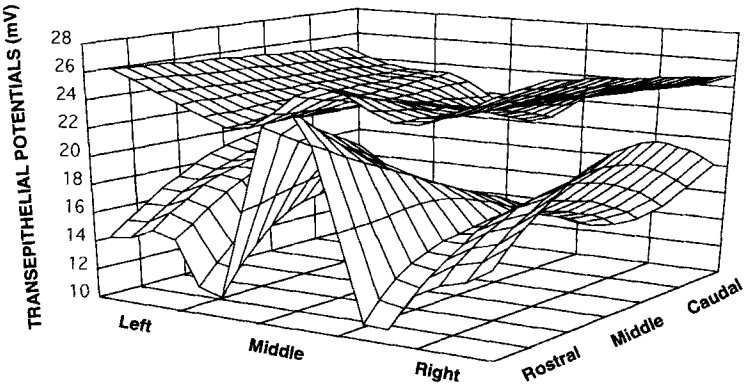

Fig. 9. Summary three-dimensional plot of TEPs at stage 15/16 and stage 18/19. At the **bottom,** the same graph as appeared in Figure 8 (for stage 15/16 embryos) is replotted alongside a similar 3-dimensional graph of all mean TEP data obtained from stage 18/19 embryos (**top graph**). The overall increase in magnitude of TEPs at stage 18/19 is real, permitting these two views to be presented adjacent to each other. Note that only a hint of the characteristic voltage gradients beneath the ectoderm is evident at stage 18/19 and these potentials are not statistically different from one another. The embryo is essentially isopotential within the extracellular domain of the neural plate near the climax of neurulation.

gradients of electrical potential within axolotl embryos. Teratological responses include deletions of structure, such as optic, otic, or olfactory primordia; misplaced or supernumerary primordia; incomplete fusion of the neural folds; and irregular development of axial symmetry (Metcalf and Borgens, 1994).

3. Application of an external field (ca. 50 mV/mm) during gastrulation, and terminating it prior to neurulation, has no effect on embryonic development (Metcalf and Borgens, 1994). Similar fields imposed across axolotl embryos for 18–24 hr beginning at the climax of neurulation (stage 19/20) also has no effect on subsequent development (Jenkins and Borgens, unpublished observations). The disruptive effects of applied voltages on axolotl development can only be produced within the window in time when endogenous fields are well expressed (stages 15–18). These experiments also demonstrate that the imposed voltage gradient has no general "toxic" effect on embryonic development, and that embryonic cells may acquire the ability to respond to extracellular voltages as orientational or directional cues sometimes after gastrulation (Metcalf and Borgens, 1994).

4. One can observe predictable effects on development when embryos are held in a fixed position within an applied electric field. When the rostral end of the embryo faced the cathode, "head" abnormalities predominated in the population, and when the caudal end faced the cathode, "tail" abnormalities predominated. Embryos held perpendicular to the long axis of the voltage gradient appeared similar to unoriented embryos showing numerous developmental abnormalities along the body axis. Moreover, the imposed field produces a predictable physiological modification of the embryonic TEP at both ends of the embryo, and the internal fields generated by it (Metcalf and Borgens, 1994).

5. We have been able to reduce the potential difference across the wall of the neural tube (the so called transneural tube potential or TNTP) in axolotl embryos. Iontophoresis of amiloride or benzamil into the neural tube lumen leads to a partial collapse of the TNTP. The developmental responses in such embryos was compared to control embryos injected with vehicle alone or to control embryos in which the same channel blockers were injected just beneath the surface ectoderm (Shi and Borgens, 1994). Control embryos developed normally but virtually all experimental embryos suffered dramatic deletions of CNS structure, incomplete cranial development, and a general de-differentiation of histological structure (Shi and Borgens, 1994). Another such demonstration of the consequences of reducing endogenous electric fields has been carried out in the stage 15 chick embryo. At this stage a very strong outwardly directed current is observed leaving the posterior intestinal portal driven by the TEP of surface ectoderm (Hotary and Robinson, 1990). This outcurrent is associated with a measured internal field of about 20 mV/mm, negative at the region of the portal with respect to more rostral sampling positions. When small conductive glass current shunts were inserted into the ectoderm near this region they produced an alternate current pathway which reduced the outcurrent at the portal by about 30%. This procedure leads to developmental defects, including major deletions of tail structure as well as other problems at more rostral regions. Control (non-conductive) shunt applications had little effect on development (Hotary and Robinson, 1992).

Finally, we have previously outlined the means by which extracellular gradients of voltage may act in concert with genetic and molecular controls in laying out embryonic form (Metcalf et al., 1994). A more complete understanding of morphogenesis will come about through investigations of the interrelationship between physiological and molecular controls of pattern formation.

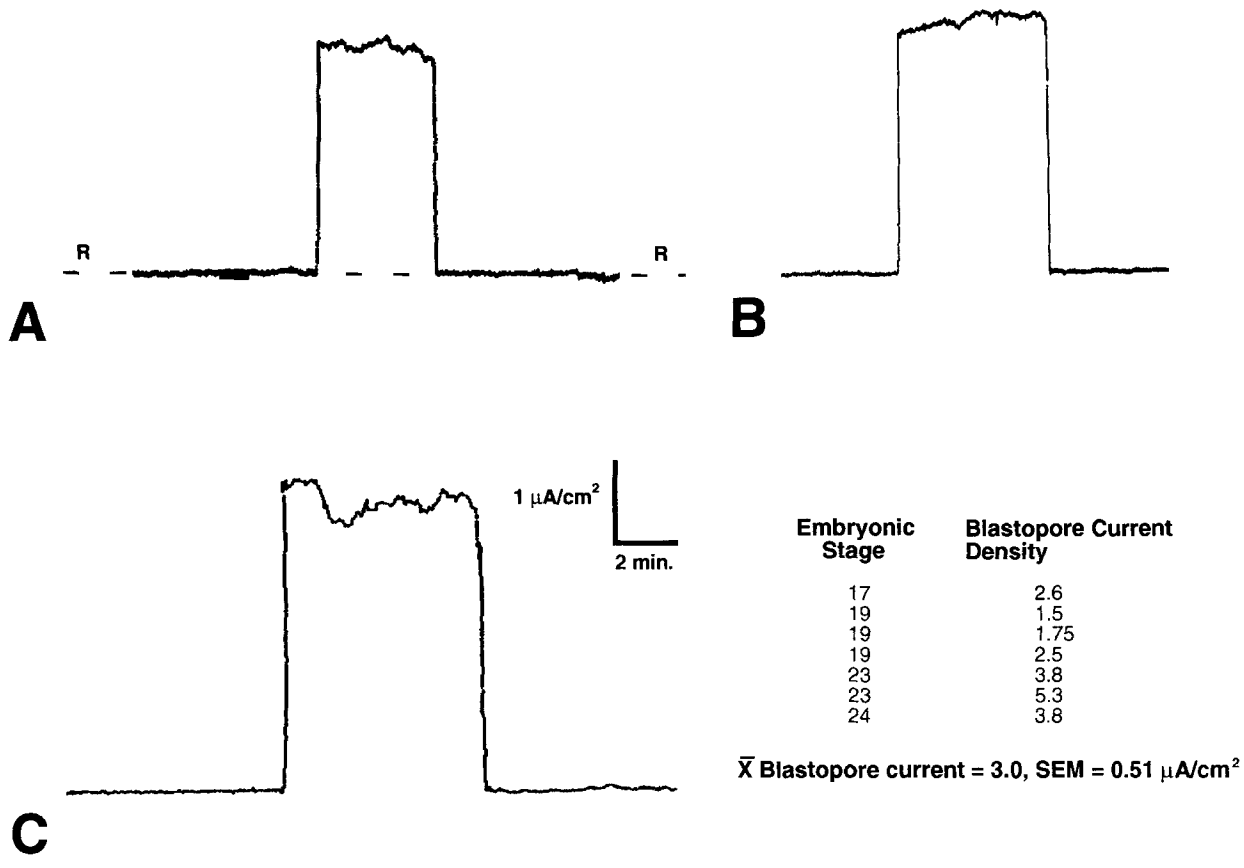

Embryonic Stage	Blastopore Current Density
17	2.6
19	1.5
19	1.75
19	2.5
23	3.8
23	5.3
24	3.8

$\bar{X}$ Blastopore current = 3.0, SEM = 0.51 μA/cm²

Fig. 10. Representative electrical records of blastopore currents in stage 17–24 embryos. A non-invasive extracellular vibrating electrode (Jaffe and Nuccitelli, 1974; Metcalf and Borgens, 1994) recorded these outwardly directed ionic currents in a stage 17 (**A**), 20 (**B**), and 24 (**C**) embryo, respectively. The dashed line is the reference position (R) where the electrode is over 1 cm from the embryo and out of the electric field. Currents were easily detected when the probe was brought into a standard measurement position ca. 50 μm from the blastopore, with the plane of vibration normal to the embryos surface at this location. Excursions of the recording pen above reference are outwardly directed currents; below reference, inwardly directed currents (though none are shown here). Note the steady current *leaving the blastopore* at all stages.

EXPERIMENTAL PROCEDURES

Most of the relevant details concerning embryo use, husbandry, and physiological measurement have been provided in previous reports in this series (Metcalf et al., 1994; Metcalf and Borgens, 1994; Shi and Borgens, 1994). We direct the reader to this description, and only provide abbreviated details here.

Embryos and Husbandry

Axolotl (*Ambystoma mexicanum*) embryos were obtained from the Indiana University Axolotl Colony as early gastrulae, and staged according to Bordzilovskaya et al. (1989). They were housed at 5°C until use when they were moved to finger bowls at room temperature in 25% Holtfreter's medium (15 mM NaCl, 0.17 mM KCl, 0.23 mM $CaCl_2$, and 0.6 mM $NaHCO_3$; pH 7.4, and resistivity 600–650 Ω cm). Physiological recordings were made with the embryos bathed in this media as well. The jelly coat and vitellin membrane were mechanically removed prior to physiological measurement.

Physiological Recording of the Transepithelial Potential

Embryos, stripped of their extraembryonic membranes, were positioned in indentations made for them in the substrate (2% Agar) of the measurement chamber and bathed in 25% Holtfreter's solution. Electrical recordings were made using unbeveled 2 meg Ω microelectrodes (100 mM NaCl filling solution, ca. 2 mV tip potentials), which were pulled on a David Kopf 700 C and later connected to standard bridge circuitry as described elsewhere (Metcalf et al., 1994; Metcalf and Borgens, 1994). Chart recordings were made on a Fisher 5000 Recorder. These chart recordings were captured to a MAC Quadra 800 computer using a LaCie Silverscanner. Microelectrode penetrations were made at particular locations on the embryos (as shown in the accompanying figures) to reveal extracellular voltage gradients in the rostral/caudal (long) axis of the midneural plate or the transverse axis. No more than eleven penetrations were made on any one embryo, which meant that a right and left matrix of sampling

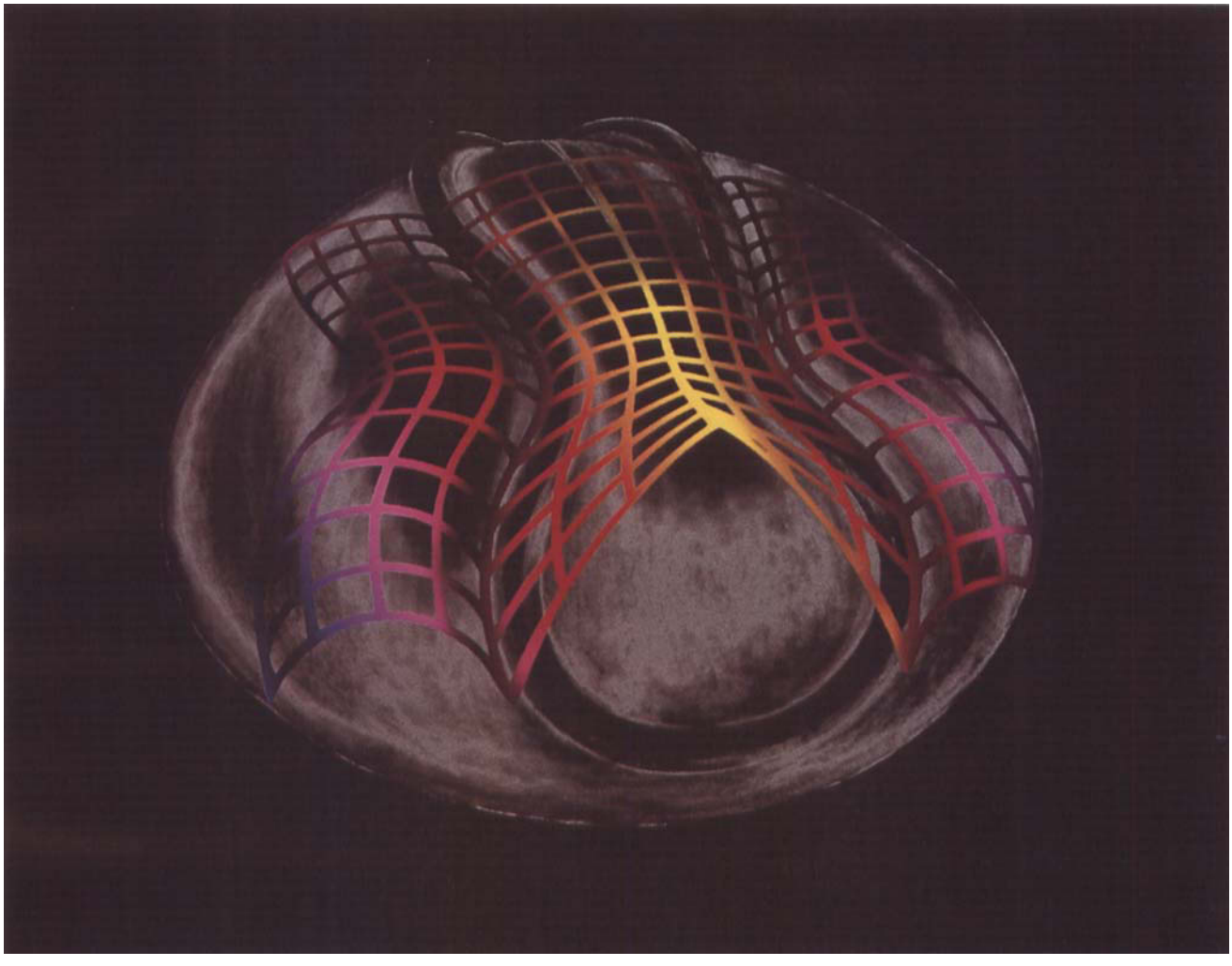

Fig. 11. Artist's reconstruction of the topography of electric fields in stage 15/16 embryos. This artist's drawing attempts to insert the general form of subectodermal voltages as shown in the three-dimensional graph (Fig. 8) within a mid-neurula amphibian embryo. This drawing helps show the relationship between the slope of internal voltages with external form of the neurula.

positions were carried out on different sets of embryos if necessary. TEP sampling at the mid-neural plate region was eliminated by the fusion of the neural folds along the dorsal midline by stage 18.

Three-Dimensional Graphic Reconstructions and Statistics

Three-dimensional graphs of transepithelial potential (TEP) were constructed using Stastica® software, in which a surface plot of voltages is obtained by a distance weighted least squares analysis producing the topography of the electrical field. Statistical evaluation between groups of TEP data was performed using a parametric test (Student's t).

ACKNOWLEDGMENTS

We acknowledge the expert technical assistance of Debra M. Bohnert and Aaron M. Harbath, financial support from the U.S. Army Medical Research and Development Command DAMD-17-91-Z-1008, and support of the Center for Paralysis Research by the Canadian Spinal Research Organization. We thank Donald Bliss and Andrea O'Shea for the fine artwork, Heather A. Eddy for manuscript preparation, and Lionel Jaffe and Andrew Blight for helpful suggestions during the conduct of these experiments.

REFERENCES

Anderson, D.J. (1992) Molecular control of neural development. In: "Molecular Neurobiology." Hall, Z.W., (ed.) Sunderland, MA: Sinauer Associates, Inc., pp 355–387.

Blackshaw, S.E. and Warner, A.E. (1976) Alterations in resting membrane properties during neural plate stages of development of the nervous system J. Physiol. (Lond.) 225:231–247.

Bordzilovskaya, N.P., Detlaff, T.A., Kuhon, S.T. and Malacinski, G.M. (1989) "Developmental Biology of the Axolotl." (Amstrong, J.B. and Malacinski, G.M. (eds) New York: Oxford University Press, pp 201–291.

Borgens, R.B., Shi, R. Mohr, T.J. and Jaeger, C.B. (1994) Mammalian

cortical astrocytes align themselves in a physiological voltage gradient. Exp. Neurology 128:41–49.

Borgens, R.B. (1992) Applied voltages in spinal cord reconstruction: history strategies, and behavioural models. In: "Spinal Cord Dysfunction, Volume III: Functional Stimulation," Illis, L.S. (ed). Oxford: Oxford University Press, pp 110–145.

Cooper, M.S. and Keller, R.E (1984) Perpendicular orientation and directional migration of amphibian neural crest cells in DC electrical fields. Proc. Natl. Acad. Sci. U.S.A. 81:160–164.

Decker, R.S. (1981) Disassembly of the zonula occludens during amphibian neurulation. Dev. Biol. 81:12–22.

Erickson, C.A. and Nuccitelli, R. (1984) Embryonic fibroblast motility and orientation can be influenced by physiological electric fields. J. Cell Biol. 98:296–307.

Hinkle, L., McCaig, C.D., and Robinson, K.R. (1981) The direction of growth of differentiating neurons and myoblasts from frog embryos in an applied electric field. J. Physiol. 314:121–135.

Hotary, K.B. and Robinson, K.R. (1990) Endogenous electrical currents and the resultant voltage gradients in the chick embryo. Dev. Biol. 140:149–160.

Hotary, K.B. and Robinson, K.R. (1992) Evidence of a role for endogenous electrical fields in chick embryo development. Development 114:985–996.

Jaffe L.F. and Nuccitelli, R. (1974) An ultrasensitive vibrating probe for measuring steady extracellular currents. J. Cell Biol. 63:614–28.

Jaffe, L.F. and Stern, C.D. (1979) Strong electrical currents leave the primitive streak of chick embryos. Science 206:569–571.

Jessell, T.M. and Melton, D.A. (1992) Diffusible factors in vertebrate embryonic induction. Cell 68:257–270.

Kirschner, L.B. (1973) Electrolyte transport across the body surface of freshwater fish and amphibia. In: "Transport Mechanisms in Epithelia." Ussing, H.H. and Thorn, N.A. (eds). Copenhagen: Munksgaard, pp 447–460.

McCaig, C.D. and Dover, P.J. (1989) On the mechanism of oriented myoblast differentiation in an applied electric field. Biol. Bull. 176: 140–144.

McCaig, C.D. and Robinson, K.R. (1982) The ontogeny of the transepidermal potential difference in frog embryos. Dev. Biol. 90:335–339.

McCaig, C.D. (1986) Dynamic aspects of amphibian neurite growth and the effects of an applied electric field. J. Physiol. 375:55–69.

Messenger, E.A. and Warner, A.E. (1979) The function of the sodium pump during differentiation of amphibian embryonic neurones J. Physiol. (Lond.) 292:85–105.

Metcalf, M.E.M. and Borgens, R.B. (1994) Weak applied voltages interfere with amphibian morphogenesis and pattern. J. Exp. Zool. 268:322–338.

Metcalf, M.E.M., Shi, R., and Borgens, R.B. (1994) Endogenous ionic currents and voltages in amphibian embryos. J. Exp. Zool. 268:307–322.

Nuccitelli, R. (1988) Physiological electric fields can influence cell motility, growth, and polarity. Adv. Cell Biol. 2:213–233.

O'Farrell, P.H. (1994) Unanimity waits in the wings. Nature 368: 188–189.

Patel, N. and Poo, M-M. (1982) Orientation of neurite growth by extracellular electric fields, J. Neurosci. 2:483–496.

Regen, C.M., and Steinhardt, R.A. (1986) Global properties of the *Xenopus* blastula are mediated by a high-resistance epithelial seal. Dev. Biol. 113:147–154.

Robinson, K.R., and Stump, R.F. (1984) Self-generated electrical currents through Xenopus neurulae. J. Physiol. 352:339.

Robinson, H.R., Bubien, J.K., Smith, P.R., and Benos, D.J. (1991) Epithelial sodium conductance in rabbit pre-implantation trophectodermal cells. Dev. Biol. 147:313–321.

Robinson, K.R. (1985) The responses of cells to electrical fields, a review. J. Cell Biol. 101:2023–2027.

Shi, R. and Borgens, R.B. (1994) Embryonic neuroepithelium sodium transport, the resulting physiological potential, and cranial development. Dev. Biol. 165:105–116.

Smith, P.R. and Benos, D.J. (1991) Epithelial Na channels. Ann. Rev. Physiol. 53:509–530.

Stern, C.D. and MacKenzie, D.O. (1983) Sodium transport and the control of epiblast polarity in the early chick embryo. J. Embryol. Exp. Morphol. 77:782–98.

Stump, R.T. and Robinson, K.R. (1983) *Xenopus* neural crest cell migration in an applied electrical field J. Cell Biol. 97:1226–1233.

Warner, A.E. (1985) Factors controlling the early development of the nervous system. In: "Molecular Bases of Neural Development," Edelman, G.E., Gall, W.E., and Cowan, W.M. (eds). New York: John Wiley & Sons, pp 11–34.

Wiley, L.M. and Nuccitelli, R. (1986) Detection of transcellular currents and effect of an imposed electric field on mouse blastomeres. In: "Ionic Currents in Development," Nuccitelli, R. (ed). New York: Alan R. Liss, pp. 197–204.

Wilson, E.B. (1925) "The Cell in Development and Heredity, 3rd edition." New York: McMillian, p 1056.